


Grey Wolf Optimization and Deep Belief Networks for Data-Efficient Forecasting in Smart Renewable Energy Systems


Abdulahdi Altherwi

(Industrial Engineering Department, College of Engineering and Computer Sciences,
Jazan University, Jazan, Saudi Arabia

 <https://orcid.org/0009-0001-3366-4917>, aaaltherwi@jazanu.edu.sa)


Md. Mottahir Alam

(Department of Computer Science and Engineering, Indian Institute of Technology Patna,
Patna 801106, India

 <https://orcid.org/0000-0003-2127-7183>, mohammad.mottahir@gmail.com)


Mastoor M. Abushaega

(Industrial Engineering Department, College of Engineering and Computer Sciences,
Jazan University, Jazan, Saudi Arabia

 <https://orcid.org/0000-0002-1877-1466>, mabushaega@jazanu.edu.sa)


Abdulmajeed Azyabi

(Industrial Engineering Department, College of Engineering and Computer Sciences,
Jazan University, Jazan, Saudi Arabia

 <https://orcid.org/0000-0002-1420-8078>, aazyabi@jazanu.edu.sa)


Ahmed Hamzi

(Industrial Engineering Department, College of Engineering and Computer Sciences,
Jazan University, Jazan, Saudi Arabia

 <https://orcid.org/0009-0002-3194-9465>, amhamzi@jazanu.edu.sa)


Shabbir Hassan

Department of Computer Sciences, Aligarh Muslim University, Aligarh, India

 <https://orcid.org/0000-0003-4015-8593>, shassan.cs@amu.ac.in)

Asif Irshad Khan

(Department of Computer Sciences, Aligarh Muslim University, Aligarh, India

 <https://orcid.org/0000-0003-1131-5350>, airshad.cs@amu.ac.in)

Abstract: The integration of hybrid renewable energy systems (HRES) has introduced both opportunities and challenges in managing multisource power systems such as wind and solar. Accurate forecasting of HRES performance is critical to efficient planning and grid stability. This paper proposes a data efficient hybrid framework that combines Grey Wolf Optimization (GWO) for feature selection with Deep Belief Networks (DBN) for predictive modeling. GWO effectively selects relevant features from high dimensional environmental and system parameters, reducing computational burden and enhancing learning performance. The DBN is then trained on the optimized input set to forecast system performance. Two public datasets capturing wind and solar power production across distinct geographic conditions were used for validation. The

proposed model significantly outperforms conventional methods, achieving a mean square error of 0.0207, RMSE of 0.144, and an energy efficiency of 98.32%. These results demonstrate the framework's potential for deployment in smart grid forecasting environments.

Keywords: Computational Intelligence, Deep Belief Network, Grey Wolf Optimization, Hybrid Renewable Energy Systems, Metaheuristic Feature Selection, Smart Grid Forecasting

Categories: H.3.1, H.3.2, H.3.3, H.3.7, H.5.1

DOI: 10.3897/jucs.160204

Abbreviation	Description
ANN_PSO	Artificial Neural Networks with Particle Swarm Optimization
ANNR_AO	Artificial Neural Network Regression with Adam Optimization
CNN	Convolutional Neural Network
DBN	Deep Belief Neural Network
DNN_PSO	Deep Neural Networks with Particle Swarm Optimization
FRL	Fuzzy Reinforcement Learning
GObNN	Genetic Optimization-based Neural Networks
GRU-RNN	Gated Recurrent Unit-Recurrent Neural Network
GWO	Grey Wolf Optimization
HMAN	Hybrid Meta-Heuristic Artificial Neural Networks
HRE	Hybrid Renewable Energy
HRES	Hybrid Renewable Energy System
KNN	K-Nearest Neighbors
MAE	Mean Absolute Error
ML	Machine Learning
MLP	Multilayer Perceptron
NREL	National Renewable Energy Laboratory
PCA	Principal Component Analysis
RMSE	Root Mean Square Error
SoC	State of Charge

Table 1: List of abbreviations

1 Introduction

Businesses and government institutions have recently increasingly utilized renewable energy systems worldwide because of their eco-friendly nature [Qureshi et al. 2022]. The increasing awareness of climate change, and greenhouse gas emissions demands a sustainable and clean energy source, which leads to the adoption of renewable energy systems [SAR et al. 2020]. The forecasting of hybrid renewable energy systems is important to ensure optimal functioning and effective energy utilization [Murugaperumal

et al. 2020]. The hybrid renewable energy system blends multiple renewable energy sources, such as solar, wind, thermal, hydro, etc., to attain reliability, and improved energy efficiency [Jurasz et al. 2019]. Recent studies have suggested that Machine Learning (ML) techniques have emerged as a powerful mechanism for forecasting the performances of hybrid renewable energy systems [Rangel-Martinez et al. 2021]. The ML-based prediction techniques influence the characteristics of ML algorithms such as regression models, decision trees, support vector machine (SVM), neural networks, etc., to learn patterns and interconnections between the data, ensuring precise predictions based on the historical and real-time data collected from the hybrid renewable energy systems [Zhu et al. 2020, Sharma et al. 2022, Farooq et al. 2021]. The ML approach examines factors like energy production, weather conditions, load demand, etc., to offer valuable insights into the expected performance of hybrid renewable energy systems [Arsad et al. 2022]. Fig. 1 illustrates the architecture of the ML-based performance prediction system in a hybrid renewable energy system.

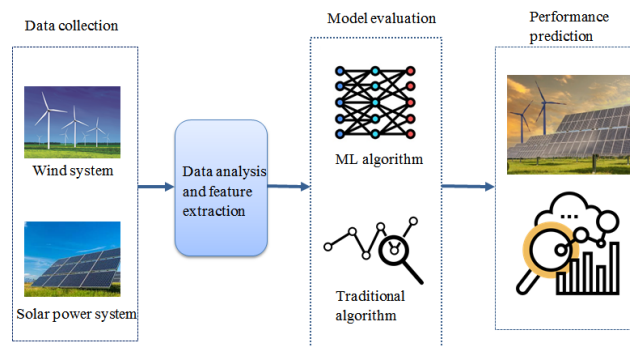


Figure 1: Architecture of ML-based prediction model

Integrating ML algorithms to forecast the performance of hybrid renewable energy systems provides various benefits [Al-Othman et al. 2022]. It helps the system to determine complex relationships and interconnections between the factors affecting the system outcomes, whereas the existing techniques face challenges in examining the complex nonlinearities and non-obvious patterns of hybrid renewable energy systems [Naik et al. 2022]. Moreover, ML techniques can process and handle massive volumes of data, enabling the system to analyze and forecast comprehensively [Li et al. 2021]. Furthermore, the introduction of ML approaches induces false positives, and false negatives (errors) in the prediction analysis because of the huge training process [Kuradusenge et al. 2020]. This results in inaccurate predictions and reduces the system's performance. Therefore, to resolve these issues in the ML-based prediction models, various optimization techniques, such as grey wolf optimization, whale optimization, etc., are integrated into the ML algorithms to optimize the training process, thereby, reducing the errors in the prediction process [Zhang et al. 2022, Lu et al. 2021, Lipu et al. 2021]. Although the integrated hybrid mechanism minimized the error and enhanced the prediction accuracy, they face challenges such as computational complexity, and scalability. Furthermore, the existing algorithms such as software model for maximum power production in energy systems

[Al-Janabi & Al-Janabi 2023], fuzzy reinforcement learning [Hasmat & Yadav 2021], improved gated recurrent unit-recurrent neural network DL-based prediction model for hybrid energy systems [Shalini & Revathi 2023], face problems like difficulty in dataset training, increased computational time, and cost, and their system performance depends on the quality of the input dataset.

HRES combines loads, storage systems, and various energy sources such as solar, wind, hydro, etc. all of which have unique dynamic conditions [Alabi et al. 2022]. Additionally, complex modelling methods are necessary due to the nonlinear and frequently poorly understood interactions among the components. Here, the systems become more complex when they are scaled up, especially in prediction and optimization models. Demand forecasts are made more unclear by the fact that user behavior affects energy consumption patterns [Ghandehariun et al. 2023]. The nonlinear and dynamic behavior of HRES is frequently not captured by linear and rule-based models. Neural networks and other predictive models are susceptible to overfitting when trained on sparse or noisy data [Bhutta et al. 2024]. Conventional optimization techniques like particle swarm optimization and evolutionary algorithms can become trapped in local optima and produce less-than-ideal predictions [Zhou et al. 2020].

To overcome these issues, this paper proposes an effective, optimized ML-based framework to predict the performances of a hybrid renewable energy system. The main contributions of the presented research work are described as follows:

- Develop a hybrid renewable energy (HRE) system and collect performance information such as solar incidence, wind speed, and power output. Then, preprocess the collected data and extract relevant features.
- Apply the fitness function of the GWO algorithm to select the optimal features from the extracted feature set; this decreases the input data dimensionality and enhances prediction efficiency.
- Train the DBN model using the selected optimal features to predict the performance of the HRE system for new input data.
- Evaluate the outcomes of the proposed framework in terms of MSE, RMSE, coefficient of determination, and accuracy, and validate the results with existing prediction algorithms.

The organization of the presented research work is sequenced as below; the research articles related to the developed framework are described in section 2, the proposed hybrid framework is explained in section 3, the outcomes of the proposed methodology were analyzed in section 4, and the research conclusion is described in section 5. Table 1 summarizes the list of abbreviations used in this paper.

2 Related Works

The remarkable evolution of various industries creates a demand for sustainable energy systems.

Currently, renewable energy sources are utilized to power the industrial sectors, and to predict the performance of the hybrid renewable energy system, many researchers have reported their works. For example [Al-Janabi & Al-Janabi 2023] presented a software design for generating maximum power from the energy system. This method

works by predicting the performance of the renewable energy system using the multi-parameter objective function of the gradient boosting algorithm. However, implementing the developed software model is complex and prone to overfitting problems.

The paper [Hasmat & Yadav 2021] proposed a wind speed prediction algorithm using fuzzy reinforcement learning (FRL) approach. Initially, the wind speed of the turbine is continuously measured using the ranker search technique. This measured wind speed acts as the input to the FRL algorithm, which forecasts the wind speed in the future. Finally, the performance of the proposed prediction framework was evaluated with traditional models. However, the robustness of the developed framework heavily depends on the availability and quality of training data.

The work [Shalini & Revathi 2023] proposed an innovative DL-based prediction model for hybrid energy systems. This model integrates the convolutional neural network (CNN) and bidirectional long short-term memory (LSTM) to accurately predict power output in the hybrid energy system. In this framework, the solar and wind power sources act as the input sources of the hybrid energy mode. The presented works were modeled in the MATLAB software, and the results are validated. However, training this integrated mode was computationally intensive.

In the paper [Xia et al. 2021], a performance prediction algorithm using the improved gated recurrent unit-recurrent neural network (GRU-RNN) is proposed. This model was developed to predict renewable energy production and electricity load using historical power production data. The improved architecture of GRU-RNN improves the training process and minimizes the computational complexity effectively. However, this method does not consider the uncertainties of renewable energy sources.

Although solar energy forms the cleanest energy source for power generation, its intermittency characteristics cause unstable functioning of the power systems. The research work [Li et al. 2020] presented a hybrid framework for forecasting solar power output. This approach integrates the attributes of CNN and LSTM to leverage uncertainties in the system, enabling accurate power prediction. This model was validated with the real-time data collected from the solar plant located in Limberg, Belgium. However, it faces interpretability because of the integration of different models.

Recently, soft-computing-based energy prediction has earned more attention because of its efficiency in addressing the intermittency characteristics of renewable energy systems. The work [Khan et al. 2020] designed a machine learning approach to predict energy consumption. This technique utilizes the SVM and multilayer perceptron (MLP) to predict energy production by examining the historical energy system data. However, this method requires a massive dataset to train the ML models, increasing the computational cost of the system.

The intermittency and unpredictable characteristics of the renewable energy system led to unstable power generation. Therefore, to resolve these issues, the authors in [El-Aziz & RMA 2022] presented a hybrid ML model to predict the power outcomes of renewable sources accurately. This developed model combines the CatBoost approach, MLP, and SVM to improve the system performance and prediction efficiency. However, this model requires continuous maintenance, and its effectiveness depends on the quality of the training dataset.

In solar power systems, energy production heavily relies on weather conditions such as rainfall, temperature, wind, humidity, etc. Chakraborty et al. [Chakraborty et al. 2023] developed an ensemble-based ML technique for predicting the power production in solar power systems, considering the intermittency and variable nature of weather conditions. The developed model was trained, validated, and tested with the real-time dataset gathered from the solar power system placed in the Eastern India region. This

method attained 96% accuracy in forecasting the solar power output. However, this model is computationally expensive, particularly when training and predicting with large datasets. Table 2 represents a Research Gap of above mentioned works in the context to their core contribution, techniques used, and associated advantages.

#	Author name	Techniques	Advantages	Research Gap
1	[Al-Janabi & Al-Janabi 2023]	Software design	Lower computational burden	Complex and prone to overfitting problems
2	[Hasmat & Yadav 2021]	FRL forecasts the wind speed in the future	Robustness of the developed framework	Heavily depends on the availability and quality of training data
3	[Shalini & Revathi 2023]	DL-based prediction model for hybrid energy systems	Higher accuracy and enhance the renewable energy system	Training this integrated mode was computationally intensive
4	[Xia et al. 2021]	GRU-RNN	Improves the training process and minimizes the computational complexity effectively	This method does not consider the uncertainties of renewable energy sources
5	[Li et al. 2020]	CNN and LSTM	This model was validated with the real-time data collected from the solar plant located in Limberg, Belgium	Faces interpretability because of the integration of different models
6	[Khan et al. 2020]	SVM and MLP	Predict energy production by examining the historical energy system data	This method requires a massive dataset to train the ML models, increasing the computational cost of the system
7	[El-Aziz & RMA 2022]	Hybrid ML model	Improve the system performance and prediction efficiency	This model requires continuous maintenance, and its effectiveness depends on the quality of the training dataset
8	[Chakraborty et al. 2023]	Ensemble-based ML technique	This method attained 96% accuracy in forecasting the solar power output	This model is computationally expensive, particularly when training and predicting with large datasets

Table 2: Research Gap

In summary, the existing investigation demonstrates that industrial sectors are moving significantly toward using renewable energy sources, with a particular emphasis on creating precise performance prediction models for hybrid systems. This shift promotes environmental sustainability and provides financial benefits that may encourage additional industry adoption. Also, the models are highlighting the necessity of sophisticated modelling methods that can precisely predict energy production from various energy sources in a range of circumstances. This involves integrating optimization methods

with ML algorithms to improve system efficiency and predictive power, etc. Because switching to renewable energy reduces operating costs and dependency on unstable fossil fuel markets, it can eventually result in cost savings.

3 Proposed GWO-DBN Model

In this paper, a hybrid GWO-DBN is proposed for the prediction of hybrid renewable energy system (HRES) performance. This method integrates the grey wolf optimization (GWO) [El-Aziz & RMA 2022] and the deep belief neural system (DBN) [Chakraborty et al. 2023]. The proposed method involves data pre-processing, feature extraction and selection, and performance prediction. Initially, the HRES performance dataset, including the environmental and system performance parameters such as solar incidence, wind speed, temperature, power output, etc., was collected and fed into the system. In the data pre-processing phase, the collected dataset was processed to eliminate errors and missing values in the dataset. This helps to enhance dataset quality and minimize training flaws. Further, the relevant features are extracted from the filtered dataset to capture important characteristics and patterns affecting system performance. The systematic structure of the proposed methodology is presented in Fig. 2. Then, the GWO fitness solution was applied

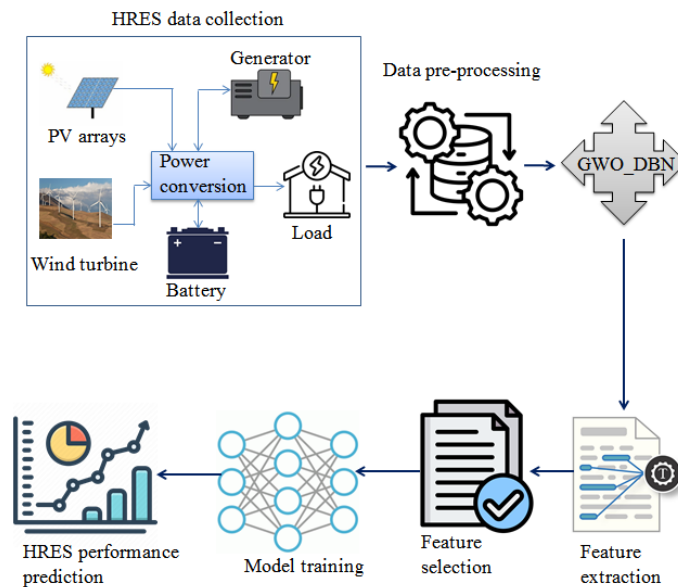


Figure 2: Proposed methodology

to select the most relevant features from the extracted features. Here, the features are extracted for initializing the fitness of each wolves and determined based on the objective function. Here, wolves move according to the search space, balancing exploitation as well as exploration functions. This helps minimize the input data's dimensionality and increases the prediction efficiency. These selected features and the corresponding system

performance data are utilized to train the DBN model. The DBN model was developed to examine the complex relationship between the input features and the system output. Moreover, before performing the DBN layer process initially identifies the input data as sequences, images, or tabular data. Then, pre-process the data and normalize the input data for handling the missing values. Then, the input layer of the DBN has neurons, so the corresponding features are allocated to each neuron. After that, verify the input dataset and neurons are equal to be in features. According to the neurons, decide the number of hidden layers to solve the complexity-dependent issues. Consequently, selects the activating function and the final output is displayed in the output layer. Thus, for each incoming input data sequence, the system predicts the performance of the HRES using the trained DBN model.

In HRES model, combining GWO with DBN paradigm can effectively increases the prediction accuracy, lowers computing complexity, permits multi-objective optimization, offers applicability across various energy sources, and strengthens system resilience. Consequently, this collaboration provides effective outcomes to contemporary energy problems while also advancing theoretical understanding. In renewable energy systems, hybridization enables the simultaneous pursuit of several goals, such as reducing power loss and increasing output efficiency performances. In a hybrid model, the GWO method may efficiently search the solution space for the best locations and dimensions for distributed generating units, enhancing system performance as a whole. GWO's versatility in optimizing DBN parameters makes it appropriate for various setups and operational circumstances, increasing its usefulness in practical applications.

3.1 System Model

The system model involves designing a hybrid renewable energy system integrating solar and wind sources. This system includes elements such as solar panels, wind turbine systems, energy storage, and power management systems. The solar energy generation module contains photovoltaic (PV) panels, which transform sunlight into electricity. The power generated by the PV module is formulated in Eq. (1) [Jallal et al. 2020].

$$P_{\text{solar}} = (A_{re}) \eta \times S_R \times S_{pf} \quad (1)$$

where P_{solar} defines the power generated by the PV module, η is denoted as solar panel's efficiency, A_{re} refers to the panel area, which denotes the surface area of the solar panels used in the PV module, S_r indicates the solar irradiance representing the intensity of sunlight, and S_{pf} denotes the solar panel efficiency indicating the ability of the solar panel to convert the sunlight into energy. Similarly, the wind turbine system's wind power is expressed in Eq. (2).

$$P_{\text{wind}} = \frac{1}{2} \times \delta \times A_d \times W_s^3 \times P_{cf} \quad (2)$$

where P_{wind} denotes the power generated by the wind turbine, δ represents the air density, A_d is denoted as swept area representation of turbine blades, W_s indicates the wind speed, and P_{cf} refers to the power coefficient. The power output of the wind turbine is primarily influenced by the wind speed and turbine-specific parameters such as swept area, power coefficient, and rotor characteristics, which define the turbine's power curve. To maintain computational tractability, the solar and wind generation models assume ideal conversion. However, real-world HRES systems experience conversion losses due to inverter inefficiencies and battery storage degradation. While these effects are not

explicitly modeled in this work, a loss coefficient η_{loss} can be introduced in future studies to capture such system-level inefficiencies.

Furthermore, although panel tilt and azimuth are implicitly captured in the dataset, architectural details such as the number of PV panels, inverter rating, and turbine rotor diameter were not available in both datasets. These variables, if provided, would allow a more detailed parametric modeling. The absence of these inputs is noted as a limitation, and future work will aim to incorporate a full physical HRES stack with sensor-driven parameterization.

The total power generated by the HRE system is the sum of energy produced by solar and wind energy systems, and it is given in Eq. (3).

$$P_{Tot} = P_{solar} + P_{wind} \quad (3)$$

where P_{Tot} denotes the total power generated by the HRE system.

Panel efficiency is assumed constant at 18%, and air density at 1.225 kg/m^3 , in accordance with standard engineering practice under nominal operating conditions. These assumptions are applied uniformly across datasets to ensure consistency in model training. While real-world conditions may introduce variability in these parameters due to temperature, altitude, or system aging, their impacts are addressed in the limitations section and earmarked for integration in future iterations of the model. Additionally, recent studies have examined predictive modeling for hybrid energy systems [Salem et al. 2022], solar photovoltaic simulation methodologies [Kumar et al. 2018], and the impact of input data variability on HRES sizing and optimization [Alberizzi et al. 2020].

In real-world environments, parameters such as air density, solar panel efficiency, and ambient temperature rarely remain constant. As a result, relying on fixed values in the energy estimation process can reduce the accuracy of the model under dynamic environmental conditions. To improve the predictive reliability of HRES forecasting, it is important to incorporate system losses and environmental variability into the model. Specifically, battery storage and inverter subsystems introduce nonlinear losses that significantly impact the usable power during energy conversion. These effects are acknowledged as limitations of the current model and are targeted for enhancement in future work.

The power generated by the HRE system is stored in batteries to balance power generation and demand. The power flow into/out of the storage module is based on the battery's state of charge (SoC). The performance prediction framework aims to forecast the outcome of the HRES based on environmental factors and historical power generation data [Khan et al. 2020]. However, the power production pattern of the power generation variation is mainly due to the inherent variability in their energy sources. The solar power is generated from the radiant energy of sunlight, which varies based on the factors like time, season, cloud, etc. On the other hand, the power production by wind power is influenced by automatic pressure, wind speed, wind directions, local weather patterns, etc. (see Fig. 3).

These two sources fluctuate over time in accordance with the climatic and atmospheric conditions. In addition, the infrastructure design also has a greater influence on power production patterns [Min et al. 2022]. The factors like solar panel count, rotor diameter, panel efficiency, etc., influence the overall power production in HRES. Therefore, understanding these factors is significant for optimizing the performance of the HRES. Hence, we developed an optimized hybrid prediction model, which examines the correlations and patterns within these parameters for accurately predicting the

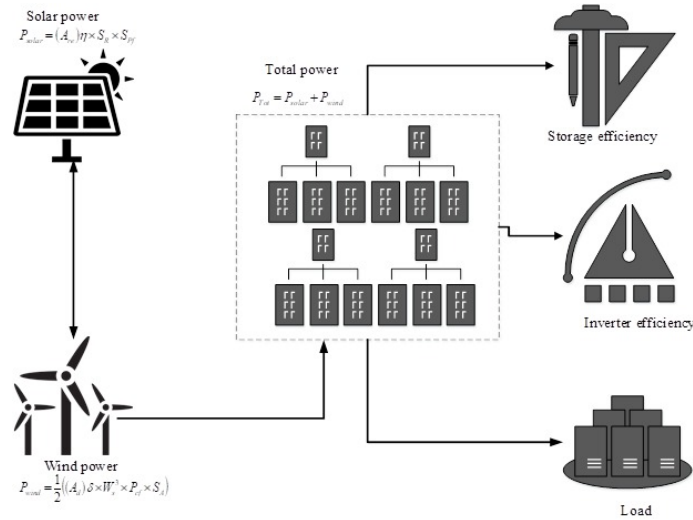


Figure 3: Modified System model

performance of HRES. This complementary nature of wind and solar power module enhances the reliability of HRES systems but needs optimal forecasting strategies to regulate its functioning for improving energy production. The prediction model should consider unique temporal and spatial dynamics of wind and solar modules for accurate forecasting. However, the existing studies have considered unified modeling approaches that fail to fully capture the distinct temporal variability and correlation patterns of wind and solar energy sources. But the proposed model considers distinct characteristics of wind and solar sources through effective feature selection, which returns fine-grained input characteristics replicating exact scenarios of wind and solar modules.

3.2 Data Collection

Initially, the hybrid renewable energy system was set up to collect the data for performance prediction. The integrated renewable energy system combines solar and wind turbine systems. The data gathering involves collecting weather, solar, wind, energy production, and historical grid data. For collecting the data on solar incidents normally includes radiation sensors which are the devices for measuring the solar energy. These are consist of spectral distribution, solar angles, solar parameters, solar irradiance, etc. moreover, quality of assurance as well as calibration is the important concerning for ensuring the accuracy of the collected data. Weather data collection includes the accumulation of weather information in the installed location of the HRES. This data includes solar irradiance, wind direction, temperature, wind speed, atmospheric pressure, humidity, etc. [Jallal et al. 2020]. The Solar data collection involves accumulating information related to solar plants such as tilt angle, orientation, number of panels, solar panel efficiency, etc. The wind data collection includes gathering information regarding the wind turbine, such as wind speed, power curves, rotor diameter, and turbulence intensity. The energy production data involves collecting historical energy production data over some time (hourly or daily measurements) from the HRES. During the data collection various

kinds of features have been recorded to categorize the solar radiations and its patterns. Here, we are taken feature like irradiance, global horizontal irradiance, diffuse horizontal irradiance, solar angles, sunshine duration, cloud cover, wind speed and that direction. The historical grid data collection includes accumulating parameters like current, power, grid demands, and other relevant measurements. This collected information is fed into the system for further processing. The mathematical formulation of data set initialization is represented in Eq. (4).

$$I_D[H_{res}] = \{D_{w1}, D_{w2}, D_{w3}, D_{w4}, \dots, D_{wd}\} \quad (4)$$

where I_D indicates the data initialization function, H_{res} refers to the collected dataset, D_w denotes the data present in the dataset, and represents the total number of data present in the dataset. This collected data may contain errors or missing values; therefore, it is important to standardize the dataset before prediction analysis.

Moreover, system representation has fundamental input variables such as panel efficiency and solar irradiance to enhance the structural factors of the additional environmental using Eq. (5).

$$E_i = S_i \cdot [\cos(\phi_n - \phi_i) \cdot \cos(\varphi - \varphi_i)] \quad (5)$$

where, ϕ_n and ϕ_i is denoted as solar incident angle as well as solar panel tilt angle respectively. Moreover, ϕ and ϕ_i is represented as solar azimuth angle as well as solar panel azimuth angle respectively. Therefore, the total power generated by the solar system is termed as Eq. (6).

$$P_{solar} = n(PV) \cdot (A_{re})\eta \times S_R \times E_i \quad (6)$$

where, $n(PV)$ is denoted as PV panels. by integrating this parameters can effectively enhances the prediction model as well as energy generation condition under varying optimization function.

3.3 Data pre-processing and Feature Extraction

Data pre-processing defines the process of cleaning the collected raw dataset by managing the missing values, noises, and errors present in it. In the developed model, the K-Nearest Neighbors (KNN) imputation approach was utilized to handle the missing values, outliers, and errors present in the input dataset. Initially address the missing values in the dataset for identifying the missing values from the irradiance data. Then, apply the KNN strategy for managing the missing data, for example removal, imputation, well as interpolation. Consequently, quality control verification is enabled or cross validate the consistency of data values. The data-pre-processing based on KNN imputation not only removes the errors but also enhances the standard and quality of the dataset. Also, smoothing filters such as gaussian filters are used to control the noise and random fluctuations from the environmental data. In addition, Z-score normalization was applied to identify the outlier which can eliminate the data points while decrease the training performance. Then strong temporal dependencies are aggregated depends upon the high frequency fluctuations which ensure the training batches while modeling the power output and energy demand system. Further, a feature extraction was performed to extract the important features from the pre-processed dataset. Here, the feature extraction was carried out using the Principal Component Analysis (PCA), which enables the system to extract important and relevant features for the prediction process. The primary objective of this algorithm is to

minimize the dimensionality of the pre-processed database while preserving the most important and significant attributes and information. Firstly, the pre-processed database is standardized to confirm that all attributes have a mean of 0 and a standard deviation of 1. Secondly, the covariance matrix of this database was determined, which captures the interconnections and relations between the present features. Further, eigenvalue decomposition was performed on the covariance matrix, which provides eigenvectors and eigenvalues. The eigenvectors indicate the directions of maximum variance in the database, while the eigenvalues measure the amount of variance offered by each eigenvector. Finally, the eigenvectors are arranged in accordance with their eigenvalues. The high eigenvalue indicates the principal element. In the proposed work, we extracted 24 features by applying the PCA technique to the pre-processed database. Then, the extracted feature sequence is fed into the feature selection module, where GWO was utilized to select the most relevant and highly significant features.

3.4 Feature Selection

Feature selection is an important step in the proposed prediction framework. In the proposed work, the feature selection step was done by applying the Grey Wolf Optimization (GWO) technique. The GWO is a nature-inspired optimization technique developed based on the social behavior of the grey wolves to solve the optimization problems. Here, it is used as main feature selection method because it demonstrates optimal exploration and exploitation abilities for high-dimensional feature spaces found in Hybrid Renewable Energy Systems (HRES) performance prediction models. The GWO utilizes its leader-based hunting mechanisms from grey wolf social hierarchy to dynamically adapt to solution landscapes while avoiding premature convergence issues and parameter tuning requirements, which is a prominent issue in GA approach. On the other hand, PSO-based feature selection model typically achieves rapid convergence yet its velocity-based update mechanism makes it vulnerable to local optima when operating in complex search spaces, which can be resolved by GWO as it exhibit greater balance between exploration and exploitation capacity. Thus, the GWO demonstrates better global search abilities which lead to its ability to find optimal feature subsets with maximum relevance and minimal redundancy. The utilization of GWO decreases the number of features in training and helps in achieving better prediction accuracy and energy efficiency. This module accepts the feature sequence containing 24 attributes as input, and processes to select the most significant attributes. The optimization begins with the initialization of the grey wolf population in which each grey wolf indicates the candidate solution for the optimization problem. In case of feature selection, the grey wolf population indicates the extracted feature sequence, and each wolf represents the subset of feature (particular feature). The primary concern of introducing this optimized feature selection model is to minimize the computational overhead of the prediction model by reducing or eliminating the irrelevant features from the database. After the initialization process, the next step is to determine the fitness value of each candidate solution. The fitness value was determined based on the objective function. The objective function is to reduce the computational overhead or training time of the prediction model. If the training time of the prediction model is low, the fitness value will be high and vice versa. The fitness solution of the GWO is expressed in Eq. (7).

$$F_{GWO}[S_{fs}] = \kappa(Ex_f) \quad (7)$$

where F_{GWO} indicates the GWO fitness solution, κ denotes the fitness function(train-

ing time), Ex_f represents the extracted feature set, and S_{f_s} refers to the selected subset of features. Training time is considered as the fitness function which can reduce the computation complex as well as enhance the computational efficiency. Here, performance of the model and predictive accuracy does not varied and minimized. Moreover, the objective function defined as to optimize the speed rather than generalizability. Also, the fitness solution of GWO refers to the fitness value of the feature subset obtained from the fitness function. After defining the fitness function, the GWO approach identifies the top three grey wolves with the highest fitness values (feature set with greater fitness values). These three grey wolves act as leaders and guide the search operation for better solutions. Further, the position of these grey wolves (α^* , β^* and γ^*) is updated and formulated in Eq. (8), (9) and (10).

$$P_{\alpha^*(n+1)} = P_{\alpha^*(n)} - \lambda * R_{\alpha^*} \quad (8)$$

$$P_{\beta^*(n+1)} = P_{\beta^*(n)} - \lambda * R_{\beta^*} \quad (9)$$

$$P_{\gamma^*(n+1)} = P_{\gamma^*(n)} - \lambda * R_{\gamma^*} \quad (10)$$

here $P_{\alpha^*(n)}$, $P_{\beta^*(n)}$ and $P_{\gamma^*(n)}$ denotes the position of α^* , β^* and γ^* in the n^* iteration in the search process, R_{α^*} , R_{β^*} and R_{γ^*} represents the random vectors, and λ denotes the coefficient, which controls the exploration process. Further, the position of other wolves (other than (α^* , β^* and γ^*)) is updated, and is expressed in Eq. (11) and (12).

$$P_{(n+1)} = P_{(n)} + \lambda (P_{\alpha^*} - (rd_1 * D_1)) + \lambda (P_{\beta^*} - (rd_2 * D_2)) + \lambda (P_{\gamma^*} - (rd_3 * D_3)) \quad (11)$$

$$P_{(n+1)}(F_{mod}) = \alpha T_e + \beta C_f \quad (12)$$

where $P_{(n+1)}$ indicates the updated position of the other wolves, $P_{(n)}$ refers to the current position of the other wolves, P_{α^*} , P_{β^*} and P_{γ^*} represents the position of α^* , β^* and γ^* . Additionally, rd_1 , rd_2 and rd_3 denotes the random vectors, which range from 0 to 1, and D_1 , D_2 and D_3 represent the direction of movement of the wolves. Moreover, $P_{(n+1)}(F_{mod})$ is denoted as modified fitness function with respect to feature vector, T_e is referred as objective value in terms of training error, C_f is represented as correlation pairwise parameter among the selected feature set and α and β is weighting factors which can balance the accuracy of the model. In this study, the values of the weighting coefficients were selected based on grid search and validation performance. The final weights were set as: $\alpha = 0.6$ (emphasizing prediction accuracy via MAE), $\beta = 0.25$ (penalizing feature redundancy), and $\gamma = 0.15$ (minimizing computational cost). These weights balance the trade-off between generalization, efficiency, and feature compactness. Here, λ are acts as a regularization balancing factors which is trade-off among the fitness function during the GWO feature selection performance. Moreover, the observed range is between 0.1 to 1.0 therefore, the computation time, selected features and model accuracy. Consequently, the main of this feature selection by applying GWO model is to predict the subset features from the original features. Therefore, minimization of computation cost as well as redundancy while improves the classification accuracy. Also, defined the

optimization objective problem using Eq. 13.

$$\max_{F_s \subseteq F} \min_{i \in E} F(F_s) = \mu A(F_s) - \nu R(F_s) - \tau |(F_s)| \tag{13}$$

$$\text{here, } \min \xrightarrow{T} \leq F_V(F_s) \leq \max \xrightarrow{T}$$

$$\text{also, } (F_s) \in \{0, 1\}^n$$

where, $F(F_s)$ is denoted as selected features set parameter representation; consequently, selected feature set such as weighting factor with respect to accuracy $\mu A(F_s)$, weighting factor with respect to redundancy $\nu R(F_s)$ and weighting factor with respect to computational cost $\tau |(F_s)|$, $\min \xrightarrow{T}$ is denoted as minimum threshold level, $\max \xrightarrow{T}$ is referred as maximum threshold level and $F_V(F_s)$ is expressed as fitness values in terms of accuracy, computation cost and timing. Thus, the position of each grey wolf in the population is updated. Moreover, it is significant to handle the feature set approximately if the updated position of the gray wolves exceeds the feature space boundaries. Here, to ensure the stable and effective convergence based on the feature selection stage, by applying the GWO algorithm. So, fitness function and search space parameters are regularized and bounded due to the binary vector which indicates 1 to selected criteria and 0 to the not selected condition. Moreover, regularization is applied via the fitness module by penalizing with larger subsets, which is $\beta(F_s)$, and redundant feature penalizing with $R(F_s)$. This regularization module is used to processed the local optima sparsity. This is obtained by restricting the position of grey wolves within the valid range. Then, estimate the fitness of the updated feature sets. If the fitness of the updated feature set is greater than the threshold value, it is selected for model training. It is formulated in Eq. (14).

$$F_s = \begin{cases} \text{Selected} & \text{if } (F_{upf} > T_{rd}) \\ \text{Not selected} & \text{else} \end{cases} \tag{14}$$

where F_s denotes the feature selection variable, F_{upf} indicates the fitness of the updated feature sets, and T_{rd} represents the threshold range of fitness value, which range between 0.9 to 1. To enhance the robustness of the feature selection process we used the empirical threshold range as 0.9, which is used for selecting the feature subset during the cross-validation interval. Here, the empirical thresholds 0.8, 0.85, 0.9, 0.95 is validated under the final selection condition for unseen data. This process is repeated continuously until the maximum number of iterations ($It\ max$) is reached. Thus, in this process, the feature set with the greatest fitness value is selected and the features with minimum fitness are discarded. This process not only reduces the computational overhead of the prediction model, but also minimizes the data dimension. In addition, this helps to improve the prediction accuracy of the model by making it easier to concentrate on the important features during the training process. These selected features serve as the input for the DBN algorithm in which the patterns and interconnections of power production can be learned to make accurate predictions. By applying the GWO-based feature selection, we selected 13 attributes from the extracted feature sequence. The selected features include solar irradiance, wind speed, wind direction, sunshine duration, cloud cover, solar panel efficiency, number of solar panels, grid humidity, wind turbine rotor diameter, solar angles (zenith angle and azimuth angle), tilt Angle of solar panels, orientation of solar panels, PV output, battery state of charge, load demand and turbulence intensity.

3.5 DBN Training

A DBN is a kind of deep learning approach, that integrates the power of unsupervised learning and deep neural networks. This is the optimal feature selection algorithm to enhance the generalization and computational efficiency and reduce the over-fitting problems. Moreover, HRE performance was integrated with this designed validation for reducing the feature space of the managed DBN's predictive accuracy. Consequently, robustness and generalization include statistical performance, model stability assessment and valuation of unseen data under the training time. Moreover, the DBN consists of multiple layers of Restricted Boltzmann Machines (RBMs) arranged on top of each other. In the proposed work, the DBN model was trained using the most relevant features selected by the GWO process. The DBN model training involves a pre-training phase, fine-tuning phase, and a performance prediction phase. The pre-training phase was designed to initialize the biases and weights of the DBN architecture. Here, each layer of the DBN is trained individually as the RBM. The energy function of the RBM is expressed in Eq. (15).

$$E_F [I_{pf}, H_d] = c^T W_t H_d - I_b^T I_{pf} - I_h H_d \quad (15)$$

here, E_F denotes the energy function, H_d refers to the hidden units, I_{pf} represents the selected input feature set, W_t defines the weight matrix interconnecting the input feature set and the hidden units, I_b refers to the input data biases, and I_h indicates the hidden units biases. The RBM training includes two phases, namely, the positive and negative phases. The positive phase of the RBM determines the activations probabilities of the hidden units applied to the input data and it is represented in Eq. (16).

$$A_{pp} = \sigma (W_t^T I_{pf} + I_h) \quad (16)$$

where A_{pp} defines the activation probabilities of the hidden units. The negative phase of RBM training estimates the reconstruction probabilities of the input feature sets, and it is formulated in Eq. (17).

$$C_{pp} = \sigma (W_t^T I_{pf} + I_b) \quad (17)$$

where C_{pp} indicates the reconstruction probabilities. Further, the weights and biases of the RBM are updated by applying the contrastive divergence approach, which is determined Eq. (18), (19) and (20).

$$W_t^* = \mu (I_{pf1} H_{d1}^T - I_{pfm} H_{dm}^T) \quad (18)$$

$$I_b^* = \mu (I_{pf1} - I_{pfm}) \quad (19)$$

$$I_h^* = \mu (H_{d1} - H_{dm}) \quad (20)$$

where W_t^* , I_b^* and I_h^* denotes the updated weight matrix, updated input feature biases, and updated hidden biases, respectively, μ refers to the learning rate, and defines the input feature set and hidden units after sampling. The pre-training was carried out in a layer-by-layer manner, iteratively from the input to the hidden layers. Once the pre-training phase was completed, the DBN model was initialized with the updated and learned weight matrix and biases for fine-tuning. This fine-tuning of the DBN design was carried out to optimize the DBN network by training it using the labeled data as a

supervised model.

The final loss function used for supervised fine-tuning of the DBN is given by Eq. (21).

$$L = \frac{1}{n} \sum_{i=1}^n (\hat{y}_i - y_i)^2 + \lambda \|W\|^2 \tag{21}$$

where, \hat{y}_i is the predicted output, y_i is the actual target value, W are the learned weight in DBN, λ is the regularization coefficient (e.g., 1×10^{-41}).

This objective function minimizes the mean squared error (MSE) while penalizing large weights via an L2 regularization term. The regularization coefficient λ was selected through grid search, with an optimal value of 1×10^{-41} that achieved the lowest validation loss. The DBN architecture is shown in Fig. 4.

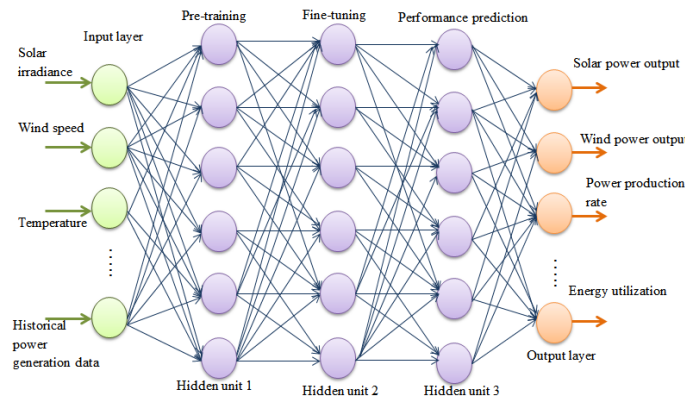


Figure 4: DBN architecture

In this phase, the DBN was entirely trained to reduce the loss function, which determines the deviation between the predicted and actual HRES performances. The loss function stating the variation between the actual and predicted performances is represented in terms of MSE and it is formulated in Eq. (22).

$$L_{S_f}^R = \frac{1}{N_s} \sum (A_p - P_p)^2 + \alpha \sum q_j^2 \tag{22}$$

where L_{S_f} indicates the loss function, N_s defines the number of training samples, A_p refers to the actual performance, and P_p denotes the predicted performance and α is denoted as a regularization coefficient function which is controlled by a magnitude squared parameter as q_j^2 . Here, mitigation of overfitting is performed DBN using the regularization term in Eq. (17). Moreover, the model was assigning the core objective generalization solution to reduce the prediction error. Also, regularization inserts the parameters that mitigates the complexity of the developed model. The gradients of the loss

function were determined and the weight matrix and biases are updated iteratively using the back-propagation approach. The trained DBN model was further utilized to predict the performances of the hybrid renewable energy system for the new input sequence. The forward pass equation for the prediction process is equated in Eq. (23).

$$L_{at1} = \rho(W_{t1}L_{at1-1} + B_{a1}) \tag{23}$$

here, L_{at1} indicates the layer 1 activation, W_{t1} represents the layer 1 weight matrix, B_{a1} refers to the layer 1 bias vector, and ρ defines the activation function.

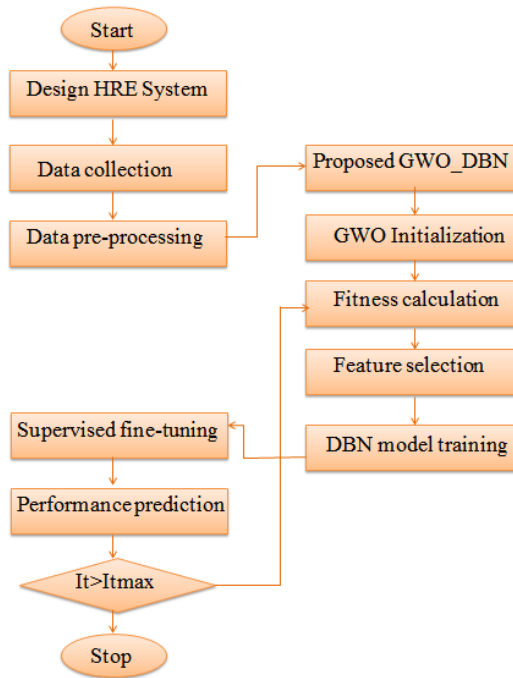


Figure 5: Flowchart of the developed model

The performance of the prediction process depends on these weight matrices, activation functions, and bias vectors. By continuously updating these parameters and predicting the performance of the HRE system accurately. Fig. 5. demonstrates the flowchart of the proposed model. Moreover, the proposed flow is explained in Algorithm 1.

4 Result and Discussion

In this article, a hybrid prediction model was developed to forecast the future performance of the HRE system based on the collected from the HRE system. This model was trained and tested with two datasets gathered from real HRES power system. The performance

Algorithm 1 HRES Power Prediction Procedure

```

1: Input: HRES database
2: Output: Total power of HRES

3: Initialization:
4:   Initialize the database
5:   Data preprocessing
6:   Feature extraction
7:   Feature selection
8: Define:
9:   Population size of GWO, maximum iterations
10:  Objective function (training time)

11: for each  $n \in l$  do
12:   Determine fitness value
13:   Sort the population based on fitness
14:   Determine alpha, beta, and delta
15:   Update the population
16:   Update fitness
17:   if updated fitness > threshold then
18:     Select feature
19:   else
20:     Discard feature
21:   end if
22: end for

23: return Selected features

24: DBN Training:
25:   Initialize DBN architecture
26:   Initialize RBM layers
27:   Initialize learning parameters
28:   Determine fitness value

29: for each training sample  $T_i$  in epoch do
30:   Initialize weights and biases
31:   Set learning rate
32:   Fine-tune DBN layers using backpropagation
33:   Determine loss  $L_j$ 
34:   Update weights  $w_i$  and biases  $b_j$ 
35: end for

36: Perform HRES performance prediction
37: Evaluate results

```

of the proposed model is then estimated in terms of MAE, RMSE, computational time, energy efficiency, etc., and validated with some existing techniques in the comparative analysis section.

4.1 Experimental Setup

The presented model was implemented in MATLAB software, version R2022b environment. All simulations and training processes were executed on a high-performance computing system equipped with an Intel Core i7 processor operating at 3.4 GHz, 32 GB of RAM and an NVIDIA RTX 3080 GPU with 10 GB VRAM.

4.2 Dataset details

The presented model was validated using two datasets. The description for two input datasets is provided below.

Dataset 1 (D1): This study used historical wind-solar power system dataset gathered using calibrated sensors installed at the Middle East Technical University (METU) from January 1, 2023 to December 26, 2023 with a sampling interval of one hour. A GPA-based Raspberry Pi module used ensures automatic collection and storage of data [Zafar et al. 2022]. This dataset consists of 8,632 samples, uniformly distributed across all four seasons, capturing significant impact of the performance of the HRES over different environmental factors. The main environmental constraints present in this dataset include wind speed, wind direction, solar irradiance, temperature, atmospheric pressure, humidity, and precipitation. This dataset is split in the ratio of 3:1 for model training and validation.

Dataset 2 (D2): Wind and Solar Daily Power Production dataset from Kaggle contains hourly records of wind and solar energy production (in megawatts) for the French electricity grid since 2020 [Wind-solar 2020]. It was created primarily to support the Commission de Régulation de l'Énergie (CRE) in calculating reference prices used in the additional remuneration system for renewable energy producers. The dataset allows various machine learning applications, including time series forecasting, anomaly detection, price signal analysis, performance benchmarking, and policy impact assessment. By leveraging features like hourly granularity, source types (wind or solar), and date/time metadata, it helps in modeling renewable energy behaviors and analyzing the effects of regulatory support mechanisms under external criteria such as weather conditions or market prices.

4.3 Performance Evaluation

In the performance evaluation section, the training and testing performance of the proposed model were analyzed. Here, the input collected dataset is split into certain ratios as, 3:1 for training, and testing purposes. Table 3 lists the training constraints.

The training accuracy defines the rate of exactly predicted values using the DBN on the training dataset. This measures how well the designed model fits the training data. The high training accuracy demonstrates that the developed model is effective in understanding and capturing the complex patterns and relationships present in the training dataset. Similarly, the testing accuracy represents the rate at which the system correctly predicts the values using the DBN on the testing data. Moreover, it illustrates how well the trained model generalizes to new incoming input data. The high testing accuracy shows that the proposed framework effectively predicts the performance of the HRES on new instances. The training and testing accuracy of the proposed framework is evaluated by increasing the number of iterations (epoch) in the system. In the GWO, initially update the position of wolves such as alpha, beta and delta, then, other wolves are randomly selecting their own search spaces. After that define the fitness function of each wolf based on the objective function. Consequently, population size, number dimensions search spaces and maximum number of iterations are updated based on the features as well as decision variables. Repeat the iteration until it reaches accurate solutions and updates the position of main and other wolves for each iterations. Finally, verify the stopping condition or convergence of each loop. Then, optimal solution is maximized or minimized based on the objective function. Moreover, to find the minimum value of cost function, then the optimization problem is minimization problem.

#	Parameters	Specifications
1	Training samples	1000
2	Hidden units	3
3	Hidden layers-1	35
4	Size of RBM layer	[8, 6]
5	Hidden layer-2	25
6	Hidden layer-3	15
7	Batch size	10
8	Learning rate	0.2
9	Activation function	Sigmoid
10	Training epochs	50
11	Training accuracy (initial)	0.25
12	Training accuracy	0.99
13	Training loss	0.60
14	Testing loss	0.72
15	Testing accuracy (initial)	0.20
16	Testing accuracy	0.98

Table 3: Training parameters

The proposed algorithms are mainly designed to find the solution that minimizes the objective function. The training and testing accuracy analysis is displayed in Fig. 6a and 6b. Here, the accuracy of training and testing data was evaluated by increasing the number of iterations (epoch) from 0 to 50. From the analysis, it is noticed that both training and testing accuracy steadily increases and reaches the maximum of 99%, and 98%, respectively. In the initial phase, the training and testing accuracy was low, which is in the range of 0.25 and 0.20, respectively. On increasing the number of iterations, the system accuracy increases; this demonstrates that the developed approach quickly learns the complex patterns on the train data and predicts the system performance effectively on the test data. On the other hand, the training and testing loss of the proposed model was analyzed to evaluate the prediction performance. The training loss defines the measure of how well the developed model fits the training data. It estimates the deviation between the actual and predicted values. The lower value of training loss indicates that the model effectively learns to make accurate performance predictions. The testing loss refers to the measure of the performance of the proposed model on the testing data. Similar to training loss, it measures the difference between the actual and predicted values in the testing dataset.

Similar to accuracy analysis, the testing and training loss is evaluated by increasing the number of epochs from 0 to 300. In the initial stage of iteration, both training and testing losses are at their maximums of 0.6 and 0.72, respectively. On increasing the number of epochs, the loss on the training and testing datasets reduces and reaches approximately 0.02 and 0.04, respectively. The training and testing loss analysis is displayed in Fig. 7a and 7b. From the accuracy and loss evaluation, it is observed that the presented model attained greater accuracy and a very minimum loss. Here, during the training stage k-fold cross validation is applied to support the better as well as consistent generalization ability towards the independent testing parameters such as RMSE, MAE and Predictive accuracy. Moreover, various input configurations are tested under the initializations as

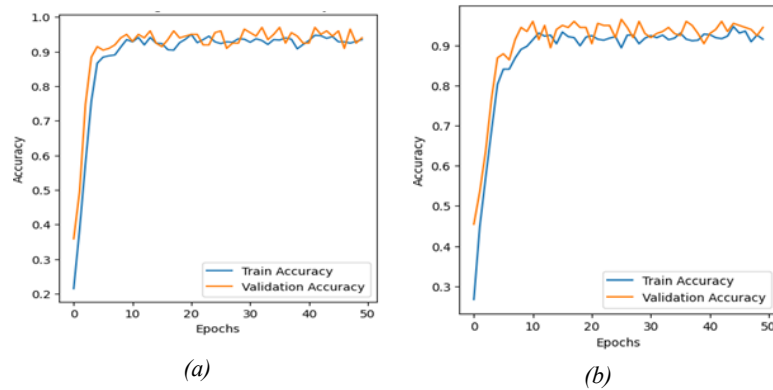


Figure 6: Accuracy performance (a) and (b)

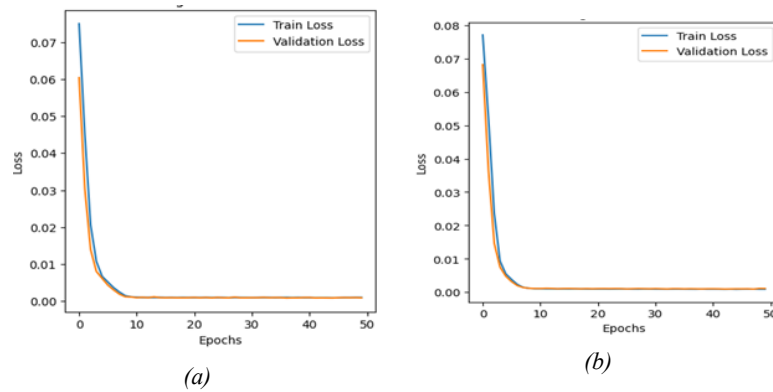


Figure 7: Training and testing loss analysis

#	Threshold	Testing accuracy
1	0.1	67.9
2	0.2	58.71
3	0.3	72.8
4	0.4	73.11
5	0.5	78.9
6	0.6	71.3
7	0.7	88.9
8	0.8	90.1
9	0.9	94.3
10	1.0	93.8

Table 4: Testing accuracy in terms of fitness thresholds

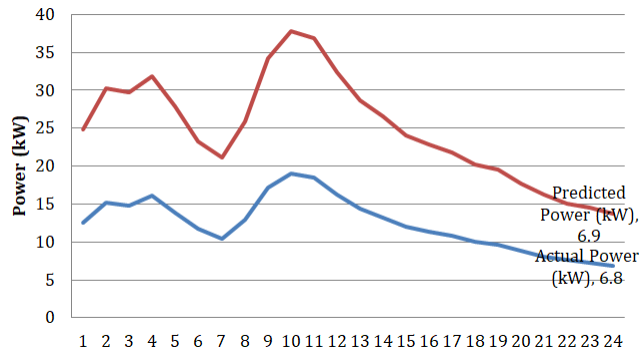


Figure 8: Actual vs. predicted power curves

well as training conditions for DBN training. This is achieved by continuously adjusting the training parameters in the proposed model.

The performance evaluation helps to assess the effectiveness and reliability of the DBN model in predicting HRES performance.

Moreover, complexity analysis is the key operation, which involves activation functions and matrix manipulation for all layers. In the asymptotic analysis the data points are considered as N layers of the DBN is represented as L , and the neuron of the largest layer is denoted as O . Therefore, the overall computational complexity is termed as $O(NLM^2)$. The time complexity is determined by the number of operations in the forward pass. For a single forward pass, it is often linear in the size of the input data.

Here, Fig. 8 mentioned the actual power with respect to the predicted power curves, this performance forecasts the time in terms of 24 hours. Moreover, the minimal prediction error was achieved for confirming the model ability. Also, Table 4 shows that the variation threshold and accuracy measurement ranges.

4.4 Comparative Assessment

In comparative assessment, the performances of the developed model such as mean absolute error (MAE), root mean square error (RMSE), coefficient of determination, energy efficiency, and computational complexity are evaluated with some existing performance prediction models. The existing approaches are utilized as comparison evaluation. Artificial Neural Networks with Particle Swarm Optimization (ANN_PSO) model is developed to control the RES in virtual power point mode [Thirunavukkarasu et al. 2023], Hybrid Meta-heuristic Artificial Neural Networks (HMANN) is developed to predict the geothermal energy day by day [Hu et al. 2020], Genetic Optimization-based Neural Networks is introduced to avoid the far possible rate and improve the ability of the distributed network (GObNN) [Manimurugan et al. 2020], Deep Neural Networks with Particle Swarm Optimization (DNN_PSO) is proposed to monitor the solar energy at different training times [Abdolrasol et al. 2021], Artificial Neural Network Regression with Adam Optimization is suggested to enhance the efficiency of prediction through the solar thermal energy (ANNR_AO) [EV Altay et al. 2022], Genetic Algorithm-assisted DBN (GA-DBN), Particle Swarm Optimized DBN (PSO-DBN), Convolutional Neural Network with Recurrent Neural Network (CNN-RNN), and Long Short-Term Memory with Genetic Algorithm (LSTM-GA).

Moreover, the selected comparative analysis models are executed under the software configurations includes, storage memory abs CPU simulation criteria based on the training performance. Also, the developed method is particularly designed for HRES application with better convergence properties, improved learning rate ability and decreased computation time.

Recent advancements in adaptive learning for dynamic environments offer complementary insights to our optimization-driven approach. For instance, the work by [Mohajer et al. 2025] presents a TD3-based reinforcement learning framework for dynamic offloading in mobile edge computing, leveraging traffic-aware network slicing to adapt in real time to fluctuating service loads. While our model focuses on predictive optimization through GWO and DBN for HRES forecasting, both approaches emphasize the importance of responsiveness under uncertainty. Incorporating policy-driven adaptation strategies, such as those enabled by TD3, could be a promising direction for enhancing model generalizability in fluctuating energy demand scenarios. Ablation analysis of the pipeline's core components is presented at the end of this section in Subsection 4.4.9.

4.4.1 MAE

MAE is a common performance evaluation metric, which defines the average absolute deviation between the actual and expected outcomes. It offers the measurement of the average magnitude of the errors computed by the proposed model. The lower rate of MAE defines greater accuracy and a closer fit between the actual and predicted performance of the HRES. The formulation of MAE is represented in Eq. (24).

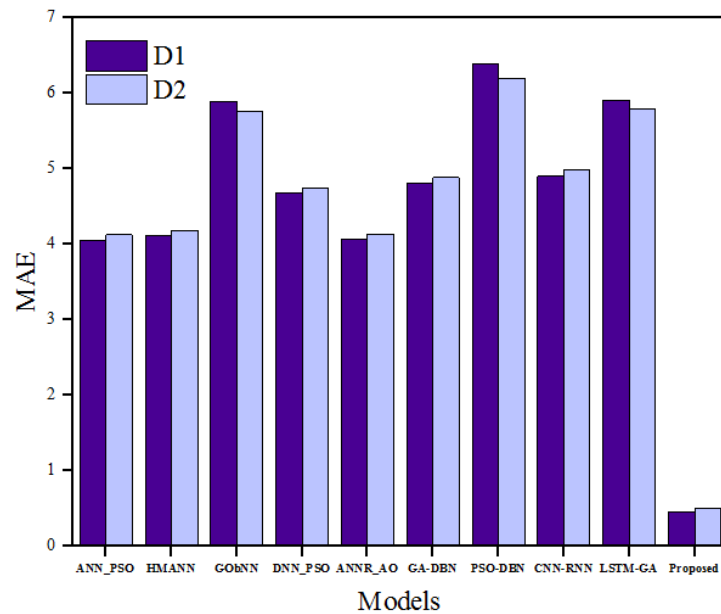


Figure 9: MAE validation

$$M_{AE} = \frac{1}{N_d} \sum |P_V - A_V| \tag{24}$$

where M_{AE} denotes the MAE, N_d refers to the total number of samples in the dataset, P_V represents the predicted outcome, and A_V indicates the actual value.

The MAE achieved by the proposed model was compared with some existing techniques such as ANN_PSO, HMANN, GOBNN, DNN_PSO, ANNR_AO, GA-DBN, PSO-DBN, CNN-RNN, and LSTM-GA. The MAE comparison is shown in Fig. 9. The MAE attained by the existing techniques is 4.056, 4.12, 5.89, 4.68, 4.07, 4.811, 6.39, 4.9 and 5.912 respectively, for D1. But the designed model earned a very low MAE of 0.457, which refers that the deviation between the actual and predicted outcomes is very small in the proposed technique. On the other hand, these existing prediction models obtained MAE of 4.123, 4.184, 5.761, 4.752, 4.131, 4.884, 6.201, 4.986 and 5.794, respectively, for D2, while the proposed model achieved a minimal MAE of 0.498. This signifies that the combination of GWO with DBN enhances the model’s prediction capacity and lowers error. The GWO algorithm narrows wide input data into a small input space by selecting only the most influential attributes, and training a DBN with these attributes reduces the prediction errors, resulting in minimal MSE.

4.4.2 RMSE

RMSE represents the square root of the average of the squared differences between the actual and predicted values. The RMSE offers the calculation of the overall accuracy of the developed model prediction. The lower value of the RMSE defines the accurate predictive performance of the proposed model. The calculation of the RMSE is formulated in Eq. (25).

$$R_{mse} = \sqrt{\frac{1}{N_d} \sum |P_V - A_V|^2} \tag{25}$$

where R_{mse} refers to the RMSE.

From the performance analysis, it is noticed that the proposed model attained a very low RMSE of 0.144. Further, to manifest the efficiency of the proposed model, the RMSE earned by the developed model is compared with existing techniques like ANN_PSO, HMANN, GOBNN, DNN_PSO, ANNR_AO, GA-DBN, PSO-DBN, CNN-RNN, and LSTM-GA. The RMSE obtained by these techniques is 3.9, 4.27, 5.91, 4.09, 4.07, 4.1, 7.2, 4.8 and 5.8 for D1, while they earned RMSE of 3.98, 4.34, 5.78, 4.18, 4.11, 4.22, 7.03, 4.89, and 5.71 for D2. But the proposed strategy earned a lower RMSE of 0.144. Among the existing techniques, the ANN_PSO obtained less RMSE compared to other approaches.

However, it is greater than the RMSE achieved by the developed model. The comparison of RMSE of different techniques is displayed in Fig. 10. The proposed algorithm achieved almost zero RMSE, indicating that the deviation between the actual and the predicted performances is relatively very small. This illustrates its effectiveness and accuracy of the developed prediction model. In addition to this, it validates that the predicted values (power production) by the developed model closely align with the actual observed values, highlighting the system’s ability to make accurate and reliable predictions. Unlike traditional prediction strategies, the GWO algorithm optimally identifies and selects only the most relevant and informative features from the datasets, which reduces deviations in

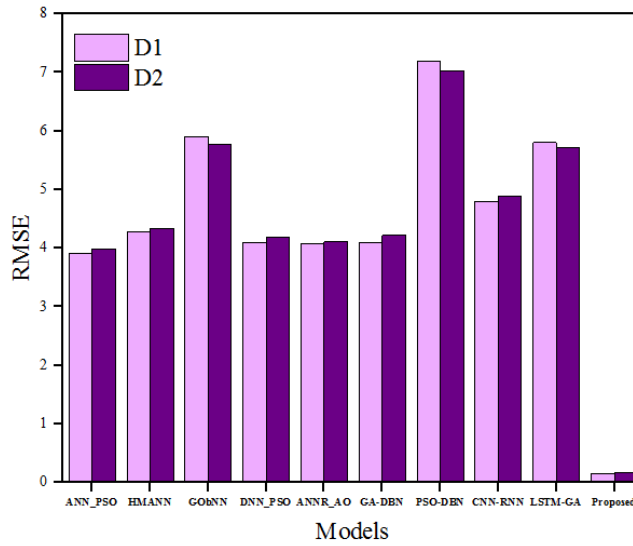


Figure 10: RMSE comparison

its training stage by allowing DBN to capture intricate and non-linear interconnections within the input sequences from the HRES systems. This results in RMSE close to zero compared to other conventional models.

4.4.3 Coefficient of Determination

The coefficient of determination R^2 is a performance metric, which defines the strength of linear interconnection between the predicted and actual system performances. The formula for the calculation of R^2 is expressed in Eq. (26).

$$R^2 = \frac{E_{ss}}{T_{ss}} \tag{26}$$

where E_{ss} indicates the explained sum of squares (ESS), and T_{ss} represents the total sum of squares (TSS). The ESS indicates the deviation in the predicted outcomes relative to the input features. It is estimated as the sum of the squared difference between the predicted and mean of the actual values. The calculation of ESS is expressed in Eq. (27).

$$E_{ss} = \sum (P_V - A_m)^2 \tag{27}$$

where A_m refers to the mean of the actual values. On the other hand, the TSS indicates the sum of squared differences between the actual value and its mean. It is expressed in Eq. (28).

$$T_{ss} = \sum (A_m - A_v)^2 \tag{28}$$

The value R^2 ranges from 0 to 1, the greater R^2 value defines the better fit of the proposed mode to the input data.

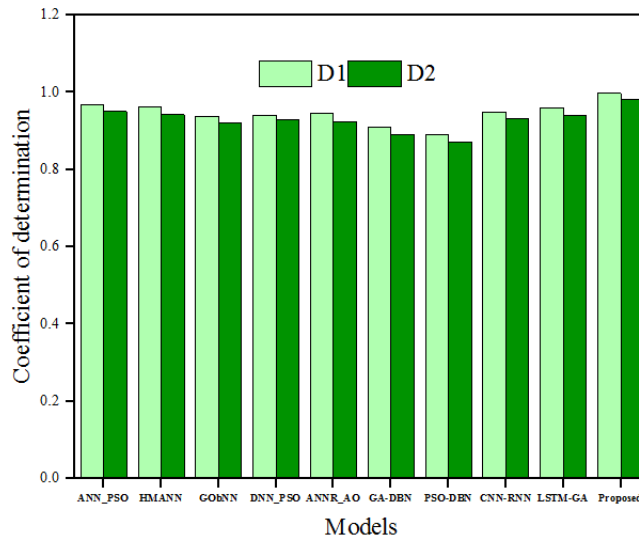


Figure 11: Validation of coefficient of determination

The validation R^2 attained by the developed model with the existing techniques is displayed in Fig. 11. The R^2 attained by the existing techniques such as ANN_PSO, HMANN, GOBNN, DNN_PSO, ANNR_AO, GA-DBN, PSO-DBN, CNN-RNN, and LSTM-GA are 0.967, 0.962, 0.938, 0.941, 0.945, 0.91, 0.89, 0.95 and 0.96, respectively for D1 dataset. Similarly for D2 dataset, these techniques achieved R^2 of 0.951, 0.942, 0.921, 0.93, 0.925, 0.89, 0.871, 0.932, and 0.94, respectively. The developed model attained a greater R^2 of 0.998 and 0.981 for D1 and D2 datasets respectively, which describes that the developed model fits the input dataset effectively and predicts the performance of the system accurately.

4.4.4 Computational Complexity

Computational complexity defines the time required by the proposed model to perform training, prediction, and optimization. This metric correlates with the resource utilization and energy efficiency of the system. The lower computational complexity represents a more efficient prediction design. The computational complexity of the proposed technique is compared with existing approaches in Fig. 12. The conventional algorithms such as ANN_PSO, HMANN, GOBNN, DNN_PSO, ANNR_AO, GA-DBN, PSO-DBN, CNN-RNN, and LSTM-GA consumed more computational time of 4.19s, 5.34s, 6.41s, 4.60s, 4.23s, 3.61s, 3.01s, 3.6s and 4.2s respectively for D1 and they consumed 5.23s, 6.47s, 7.1s, 5.37s, 5.21s, 4.2s, 4.6s, 3.74s, and 5.4, respectively for D2. But the developed model consumed very less computational time of 1.17s and 1.22s for D1 and D2 datasets. This reduction in computational time is because of the optimal feature selection, which significantly minimized the training time of the DBN model.

The comparison of training time depicts that the presented model consumed less time of 0.5s and 0.7s for DBN training, while other conventional models consumed high training time of 2.1s, 2.7s, 3.91s, 2.05s, 2.23s, 1.91s, 1.8s, 3.3s, and 2.2s, respectively for D1 dataset. Also, they consumed 2.23s, 2.93s, 4.1s, 3.0s, 2.61s, 2.2s, 2.0s, 3.4s, and

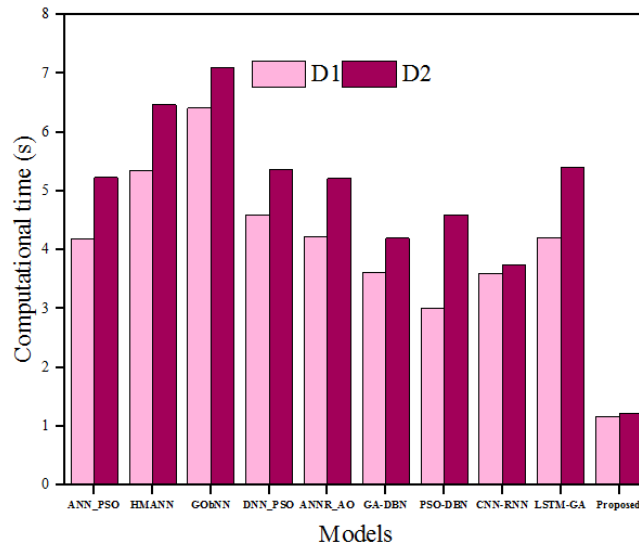


Figure 12: Evaluation of computational time

2.4, respectively for training using D2 dataset. This validates that compared to existing prediction algorithms, the designed model (GWO-DBN) consumed less time. This significant reduction is due to the feature/input space deduction by the GWO, making the DBN training simpler and efficient. Table 5 illustrates the training time of different models.

Techniques	D1	D2
ANN_PSO	2.1	2.23
HMANN	2.7	2.93
GObNN	3.91	4.1
DNN_PSO	2.05	3
ANNR_AO	2.23	2.61
GA-DBN	1.91	2.2
PSO-DBN	1.8	2
CNN-RNN	3.3	3.4
LSTM-GA	2.2	2.4
GWO-DBN (Proposed)	0.5	0.7

Table 5: Comparison of training time

4.4.5 Energy Efficiency

Energy efficiency indicates the effectiveness of the HRES in converting available energy resources (wind and solar energy) into usable electrical power. It measures the ratio of the actual energy output of the HRES to the total energy input from renewable sources. The formula for determining energy efficiency of the system is expressed in Eq. (29).

$$En_{ff} = \left(\frac{E_u}{E_T} \right) \times 100 \tag{29}$$

Where E_T indicates available energy resources, and E_u refers to usable electrical power.

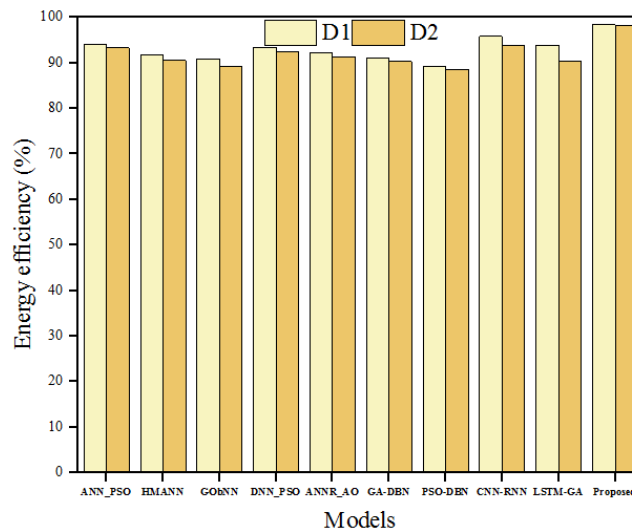


Figure 13: Energy efficiency comparison

The energy efficiency of the designed model is evaluated by comparing it with some conventional performance prediction techniques. The validation of energy efficiency is illustrated in Fig. 13. Here, the existing techniques like ANN_PSO, HMANN, GOBNN, DNN_PSO, ANNR_AO, GA-DBN, PSO-DBN, CNN-RNN, and LSTM-GA these techniques attained 93.97%, 91.79%, 90.93%, 93.42%, 92.17%, 91%, 89.20%, 95.8% and 93.88% in energy efficiency, respectively for D1 and they consumed energy efficiency of 93.23%, 90.47%, 89.1%, 92.37%, 91.21%, 90.24%, 88.6%, 93.74% and 90.4%, respectively. However, the developed model achieved an energy efficiency of 98.32% and 98.22%, which is greater than the existing techniques. The accurate prediction of HRES performance prediction enables the power providers to optimally allocate available resources to the users, resulting in enhanced energy efficiency.

4.4.6 Prediction Accuracy

The accuracy metric measures how precisely the developed algorithm predicts the performance of the HRES. The higher accuracy value suggests better prediction made by the system. Here, we compare with the existing models to validate how well the proposed technique predicts the HRES performances (generated solar and wind power). The existing models used for comparative analysis include ANN_PSO, HMANN, GOBNN, DNN_PSO, ANNR_AO, GA-DBN, PSO-DBN, CNN-RNN, LSTM-GA, and LSTM-GA. These mod-

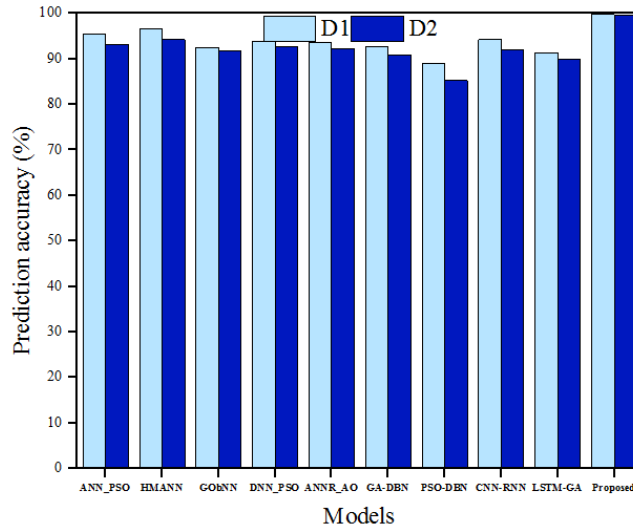


Figure 14: Accuracy comparison

els obtained accuracy of 95.45%, 96.7%, 92.53%, 93.91%, 93.56%, 92.62%, 88.91%, 94.2% and 91.33% respectively, while the proposed strategy achieved higher accuracy of 99.74%. On the other hand for D2, these existing models and the proposed strategy obtained accuracy of 93.12%, 94.18%, 91.76%, 92.75%, 92.13%, 90.88%, 85.2%, 91.98%, 89.79%, and 99.49%, respectively. Fig. 14 presents the comparison of accuracy.

From this analysis, it is clear that the proposed approach accurately predicts the HRES performance than the conventional models. By leveraging the integrated GWO and DBN, the developed algorithm demonstrates superior performance in forecasting the HRES performances.

4.4.7 Mean Square Error

Measures the average squared difference between the predicted values and the actual values. Lower MSE indicates better model performance. The formula for calculating the MSE is provided in Eq. (30).

$$\text{MSE} = \frac{1}{N_d} \sum_{i=1}^{N_d} (P_V - A_V)^2 \quad (30)$$

Models	D1	D2
ANN_PSO	15.21	17.23
HMANN	18.22	19.1
GObNN	34.89	36.4
DNN_PSO	16.73	17.37
ANNR_AO	23.91	25.21
GA-DBN	24	27.24
PSO-DBN	34.8	38.6
CNN-RNN	22.82	25.74
LSTM-GA	45.89	46.4
GWO-DBN (Proposed)	0.0207	0.025

Table 6: MSE comparison

To validate that the proposed approach obtained minimum MSE, it is compared and validated with the existing techniques like ANN_PSO, HMANN, GObNN, DNN_PSO, ANNR_AO, GA-DBN, PSO-DBN, CNN-RNN, and LSTM-GA. These conventional models obtained MSE of 15.21, 18.22, 34.89, 16.73, 23.91, 24, 34.8, 22.82 and 45.89 respectively, while the proposed approach obtained a minimum MSE of 0.0207. Subsequently, for dataset 2, these models obtained MSE of 17.23, 19.1, 36.4, 17.37, 25.21, 27.24, 38.6, 25.74, 46.4 and 0.025, respectively. This illustrates that the developed algorithm precisely predicts the HRES performances and the deviation between the actual and predicted values is relatively small. Comparison of MSE is shown in Table 6.

From the comparative assessment, it is revealed that the proposed model earned greater efficiency and minimized the deviation between the actual and predicted performances. Furthermore, the performance enhancement score is also determined to find the effectiveness of the proposed model.

4.4.8 Mean Absolute Percentage Error

MAPE measures the prediction accuracy as a percentage by comparing the absolute difference between actual and predicted values to the actual values and it is formulated in Eq. (31).

$$\text{MAPE} = \frac{1}{N_d} \sum_{i=1}^{N_d} \left| \frac{A_V - P_V}{A_V} \right| \quad (31)$$

Existing models including ANN_PSO, HMANN, GObNN, DNN_PSO, ANNR_AO, GA-DBN, PSO-DBN, CNN-RNN, and LSTM-GA obtained MAPE of 4.55%, 3.3%, 7.47%, 6.09%, 6.44%, 7.38%, 11.09%, 5.8% and 8.67%, respectively, for D1 and they earned MAPE of 5.43%, 3.89%, 8.62%, 7.19%, 7.94%, 8.75%, 13.6%, 6.5% and 9.87%, respectively for D2 dataset. But the proposed model obtained minimal MAPE of 0.26% and 0.34%, respectively, for D1 and D2 datasets. Fig. 15. displays the comparative analysis of MAPE. This illustrates that the deviation between the actual performance of HRES and the predicted performance by GWO-DBN model is minimum and negligible, highlighting the efficiency of combining GWO into DBN.

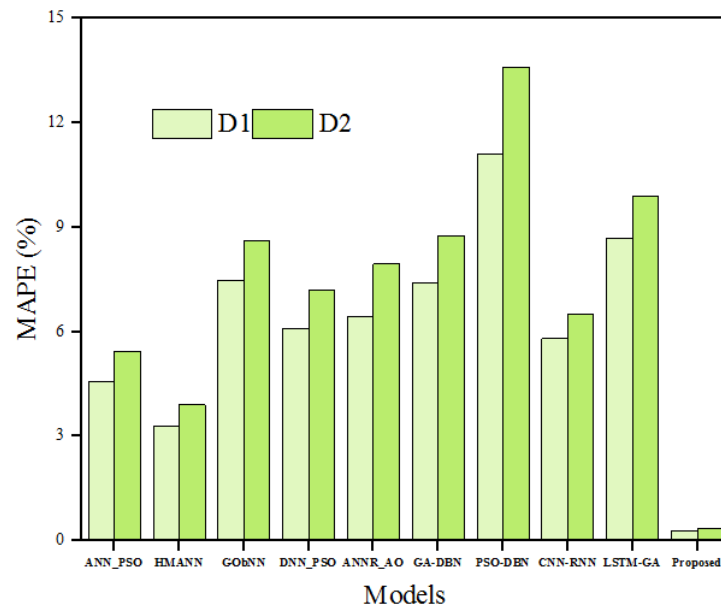


Figure 15: Comparison of MAPE with existing models

4.4.9 Ablation Analysis

To evaluate the contribution of individual components in our framework, we conducted a qualitative ablation study comparing three configurations: (i) DBN trained on raw features (baseline), (ii) DBN with PCA-based dimensionality reduction but without GWO (PCA-DBN), and (iii) the full pipeline combining GWO-based feature selection and PCA before DBN training. This comparative setup was tested on both datasets (D1 and D2) using identical preprocessing and training conditions.

Empirically, the full GWO-PCA-DBN configuration consistently yielded lower prediction errors and faster convergence than the other two variants. The use of PCA alone improved the DBN's generalization by reducing input noise and dimensionality. Adding GWO further enhanced the model's robustness by prioritizing high-correlation, high-relevance features while suppressing redundancy. This modular design demonstrates that each component meaningfully contributes to overall performance, even without presenting exact error deltas.

4.5 Discussion

The study develops a novel hybrid prediction replica that integrates GWO and DBN frameworks thoroughly investigated in the context of HRES. Although earlier research has used DBN for predictive modelling or GWO for optimization tasks independently. Here, this paper presents integration that improves predicted accuracy by utilizing the advantages of both approaches. This work particularly uses GWO to extract the most pertinent characteristics from the collected dataset, in contrast to conventional approaches that might use generic feature selection algorithms. By concentrating on the factors

that have the most effects on HRES performance, this strategy not only lowers data dimensionality but also improves model efficiency and accuracy. The statistical analysis of the comparative assessment is tabulated in Table 7. Moreover, cost saving is one of the most important performance for validating the operational cost in terms of renewable energy sources. The developed framework has 30% reduction of operational cost for optimizing the energy storage usage. This lower computation cost also lowers the feature dimensionality by approximately 22% during the training stage and attained higher prediction accuracy which has no cumulative savings such as data managing, energy cost optimization.

This study assumes constant panel efficiency $\eta = 18\%$ and air density $\rho = 1.225 \text{ kg/m}^3$ for solar and wind power calculations. While this simplification aids model consistency and reproducibility, it may introduce minor inaccuracies in real-world deployments where efficiency varies with temperature, soiling, and aging, and where air density is affected by altitude or weather. In future work, we plan to incorporate **adaptive η and ρ estimation** using sensor inputs or climate-aware models. Additionally, integrating a dynamic inverter/battery loss profile and environmental degradation factors could further improve forecasting realism.

Technology	MAE	RMSE	R ²	CT [†]	TT [‡]	EE*	PA [§]	MSE	MAPE
ANN_PSO	4.09	3.94	0.959	4.71	2.165	93.6	4.09	15.21	4.55
HMANN	4.152	4.305	0.952	5.905	2.815	91.13	4.152	18.22	3.3
GObNN	5.825	5.845	0.9295	6.755	4.005	90.02	5.825	34.89	7.47
DNN_PSO	4.716	4.135	0.9355	4.985	2.525	92.89	4.716	16.73	6.09
ANNR_AO	4.101	4.09	0.935	4.72	2.42	91.69	4.101	23.91	6.44
PSO-DBN	4.8475	4.16	0.9	3.905	2.055	90.62	4.8475	34	7.38
GA-DBN	6.295	7.115	0.885	3.805	1.9	88.9	6.295	34.8	11.09
CNN-RNN	4.943	4.845	0.941	3.67	3.35	94.77	4.943	22.82	5.8
LSTM-GA	5.853	5.755	0.95	4.8	2.3	92.14	5.853	45.89	8.67
Proposed	0.4775	0.144	0.9895	1.195	0.6	98.32	0.4775	0.0207	0.26

[†] Computational Time (seconds), [‡] Training Time (%), * Energy Efficiency (%), [§] Predictive Accuracy (%)

Table 7: Statistical analysis of comparison assessment of average performance of different models

5 Conclusion

This paper presents an intelligent forecasting model that integrates Grey Wolf Optimization (GWO) with Deep Belief Networks (DBN) for accurate and data-efficient prediction of Hybrid Renewable Energy System (HRES) performance. The GWO algorithm selects the most informative features, significantly reducing dimensionality and computational time, while the DBN model learns complex patterns from the selected input. Compared to state-of-the-art approaches including ANN_PSO, HMANN, GOBNN, and LSTM-GA, the proposed model demonstrates superior performance with lower MAE and RMSE, higher accuracy, and reduced training time. This suggests that the model can be effectively deployed for energy forecasting in smart grid operations. Future work will address limitations such as model interpretability, data-dependency, and adaptation to dynamically changing environmental conditions. Enhancing the framework with federated learning and explainable AI can further improve its applicability in decentralized and privacy-sensitive energy management scenarios.

Data Availability Statement Datasets analysed in this study are publicly available. Dataset 1 is collected via calibrated sensors at METU, and Dataset 2 is available on Kaggle at: <https://www.kaggle.com/datasets/henriupton/wind-solar-electricity-production>.

Conflict of Interest The authors have no conflict of interest to declare.

References

- [Abdolrasol et al. 2021] Abdolrasol MGM, Mohamed R, Hannan MA, Al-Shetwi AQ, Mansor M, Blaabjerg F (2021). Artificial neural network based particle swarm optimization for microgrid optimal energy scheduling. *IEEE Transactions on Power Electronics*, 36(11): 12151-12157.
- [Alabi et al. 2022] Alabi, T. M., Aghimien, E. I., Agbajor, F. D., Yang, Z., Lu, L., Adeoye, A. R., Gopaluni, B. (2022). A review on the integrated optimization techniques and machine learning approaches for modeling, prediction, and decision making on integrated energy systems. *Renewable Energy*, 194: 822-849.
- [Alberizzi et al. 2020] Alberizzi, J. C., Frigola, J. M., Rossi, M., Renzi, M. (2020). Optimal sizing of a Hybrid Renewable Energy System: Importance of data selection with highly variable renewable energy sources. *Energy Conversion and Management*, 223: 113303.
- [Al-Janabi & Al-Janabi 2023] Al-Janabi S, Al-Janabi Z (2023). Development of deep learning method for predicting DC power based on renewable solar energy and multi-parameters function. *Neural Computing and Applications*, 35: 15273-15294.
- [Al-Othman et al. 2022] Al-Othman A, Tawalbeh M, Martis R, Dhou S, Orhan M, Qasim M, Ghani Olabi A (2022). Artificial intelligence and numerical models in hybrid renewable energy systems with fuel cells: Advances and prospects. *Energy Conversion and Management*, 253: 115154.
- [Arsad et al. 2022] Arsad A, Hannan M, Al-Shetwi AQ, Mansur M, Muttaqi K, Dong Z, Blaabjerg F (2022). Hydrogen energy storage integrated hybrid renewable energy systems: A review analysis for future research directions. *International Journal of Hydrogen Energy*, 47(39): 17285-17312.
- [Bhutta et al. 2024] Bhutta, M. S., Li, Y., Abubakar, M., Almasoudi, F. M., Alatawi, K. S. S., Altimania, M. R., Al-Barashi, M. (2024). Optimizing solar power efficiency in smart grids using hybrid machine learning models for accurate energy generation prediction. *Scientific Reports*, 14.1: 17101.

- [Chakraborty et al. 2023] Chakraborty D, Mondal J, Barua HB, Bhattacharjee A (2023). Computational solar energy-ensemble learning methods for prediction of solar power generation based on meteorological parameters in eastern India. *Renewable Energy Focus*, 44: 277-294.
- [El-Aziz & RMA 2022] El-Aziz, RMA (2022). Renewable power source energy consumption by hybrid machine learning model. *Alexandria Engineering Journal*, 61(12): 9447-9455.
- [EV Altay et al. 2022] EV Altay, Gurgenc E, Altay O, Dikici A (2022). Hybrid artificial neural network based on a metaheuristic optimization algorithm for the prediction of reservoir temperature using hydrogeochemical data of different geothermal areas in Anatolia (Turkey). *Geothermics*, 104: 102476.
- [Farooq et al. 2021] Farooq F, Ahmed W, Akbar A, Aslam F, Alyousef R (2021). Predictive modeling for sustainable high-performance concrete from industrial wastes: A comparison and optimization of models using ensemble learners. *Journal of Cleaner Production*, 292: 126032.
- [Ghandehariun et al. 2023] Ghandehariun, Samane, Amir M. Ghandehariun, and Nima Bahrami Ziabari (2023). Performance prediction and optimization of a hybrid renewable-energy-based multigeneration system using machine learning. *Energy*, 282: 128908.
- [Hasmat & Yadav 2021] Hasmat M, Yadav AK (2021). A novel hybrid approach based on relief algorithm and fuzzy reinforcement learning approach for predicting wind speed. *Sustainable Energy Technologies and Assessments*, 43: 100920.
- [Hu et al. 2020] Hu P, Pan J, Chu S (2020). Improved binary grey wolf optimizer and its application for feature selection. *Knowledge-Based Systems*, 195: 105746.
- [Jallal et al. 2020] Jallal MA, Chabaa S, Zeroual A (2020). A novel deep neural network based on randomly occurring distributed delayed PSO algorithm for monitoring the energy produced by four dual-axis solar trackers. *Renewable Energy*, 149: 1182-1196.
- [Jurasz et al. 2019] Jurasz J, Canales F, Kies A, Guezgouz M, Beluco A (2019). A review on the complementarity of renewable energy sources: Concept, metrics, application and future research directions. *Solar Energy*, 195: 703-724.
- [Khan et al. 2020] Khan PW, Byun Y, Lee S, Kang D, Kang J, Park H (2020). Machine learning-based approach to predict energy consumption of renewable and nonrenewable power sources. *Energies*, 13(18): 4870.
- [SAR et al. 2020] Khan SAR, Zhang Y, Kumar A, Zavadskas E, Streimikiene D (2020). Measuring the impact of renewable energy, public health expenditure, logistics, and environmental performance on sustainable economic growth. *Sustainable Development*, 28(4): 833-843.
- [Kumar et al. 2018] Kumar, Raj, and S. K. Singh (2018). Solar photovoltaic modeling and simulation: As a renewable energy solution. *Energy Reports*, 4: 701-712.
- [Kuradusenge et al. 2020] Kuradusenge M, Kumaran S, Zennaro M (2020). Rainfall-induced landslide prediction using machine learning models: The case of Ngororero district, Rwanda. *International Journal of Environmental Research and Public Health*, 17(11): 4147.
- [Li et al. 2020] Li G, Xie S, Wang B, Xin J, Li Y, Du S (2020). Photovoltaic power forecasting with a hybrid deep learning approach. *IEEE Access*, 8: 175871-175880.
- [Li et al. 2021] Li W, Chai Y, Khan F, Jan SRU, Verma S, Menon VG, Kavita, Li X (2021). A comprehensive survey on machine learning-based big data analytics for IoT-enabled smart healthcare system. *Mobile Networks and Applications*, 26: 234-252.
- [Lipu et al. 2021] Lipu MSH, Hannan M, Karim TF, Hussain A, Saad MHM, Ayob A, Miah MS, Indra Mahlia T (2021). Intelligent algorithms and control strategies for battery management system in electric vehicles: Progress, challenges and future outlook. *Journal of Cleaner Production*, 292: 126044.
- [Lu et al. 2021] Lu P, Ye L, Zhao Y, Dai B, Pei M, Tang Y (2021). Review of meta-heuristic algorithms for wind power prediction: Methodologies, applications and challenges. *Applied Energy*, 301: 117446.

- [Manimurugan et al. 2020] Manimurugan S, Al-Mutairi S, Aborokbah MM, Chilamkurti N, Ganesan S, Patan R (2020). Effective attack detection in internet of medical things smart environment using a deep belief neural network. *IEEE Access*, 8: 77396-77404.
- [Min et al. 2022] Min D, Song Z, Chen H, Wang T, Zhang T (2022). Genetic algorithm optimized neural network based fuel cell hybrid electric vehicle energy management strategy under start-stop condition. *Applied Energy*, 306: 118036.
- [Mohajer et al. 2025] A. Mohajer, J. Hajipour and V. C. M. Leung (2025). Dynamic Offloading in Mobile Edge Computing with Traffic-Aware Network Slicing and Adaptive TD3 Strategy, in *IEEE Communications Letters*, vol. 29, no. 1, pp. 95-99.
- [Murugaperumal et al. 2020] Murugaperumal K, Srinivasn S, Prasad GRKDS (2020). Optimum design of hybrid renewable energy system through load forecasting and different operating strategies for rural electrification. *Sustainable Energy Technologies and Assessments*, 37: 100613.
- [Naik et al. 2022] Naik BT, Hashmi MF, Bokde ND (2022). A comprehensive review of computer vision in sports: Open issues, future trends and research directions. *Applied Sciences*, 12(9): 4429.
- [Qureshi et al. 2022] Qureshi F, Yusuf M, Kamyab H, Vo D-VN, Chelliapan S, Joo S-W, Vasseghian Y (2022). Latest eco-friendly avenues on hydrogen production towards a circular bioeconomy: Currents challenges, innovative insights, and future perspectives. *Renewable and Sustainable Energy Reviews*, 168: 112916.
- [Rangel-Martinez et al. 2021] Rangel-Martinez D, Nigam, K, Ricardez-Sandoval LA (2021). Machine learning on sustainable energy: A review and outlook on renewable energy systems, catalysis, smart grid and energy storage. *Chemical Engineering Research and Design*, 174: 414-441.
- [Salem et al. 2022] Salem H, Kabeel A, El-Said EM, Elzeki OM (2022). Predictive modelling for solar power-driven hybrid desalination system using artificial neural network regression with Adam optimization. *Desalination*, 522: 115411.
- [Shalini & Revathi 2023] Shalini TA, Revathi BS (2023). Hybrid power generation forecasting using CNN based BILSTM method for renewable energy systems. *Automatika*, 64(1): 127-144.
- [Sharma et al. 2022] Sharma A, Mukhopadhyay T, Rangappa SM, Seingchin S, Kushvaha V (2022). Advances in computational intelligence of polymer composite materials: Machine learning assisted modeling, analysis and design. *Arch Computat Methods Eng*, 29: 3341-3385.
- [Thirunavukkarasu et al. 2023] Thirunavukkarasu M, Sawle Y, Lala H (2023). A comprehensive review on optimization of hybrid renewable energy systems using various optimization techniques. *Renewable and Sustainable Energy Reviews*, 176: 113192.
- [Wind-solar 2020] Wind-solar & power production dataset accessed at <https://www.kaggle.com/datasets/henriupton/wind-solar-electricity-production>
- [Xia et al. 2021] Xia M, Shao H, Ma X, Silva CWD (2021). A stacked GRU-RNN-based approach for predicting renewable energy and electricity load for smart grid operation. *IEEE Transactions on Industrial Informatics*, 17(10): 7050-7059.
- [Zafar et al. 2022] Zafar, Muhammad Hamza, Noman Mujeeb Khan, Majad Mansoor, Adeel Feroz Mirza, Syed Kumayl Raza Moosavi, and Filippo Sanfilippo (2022). Adaptive ML-based technique for renewable energy system power forecasting in hybrid PV-Wind farms power conversion systems. *Energy Conversion and Management*, 258: 115564.
- [Zhang et al. 2022] Zhang W, Gu X, Tang L, Yin Y, Liu D, Zhang Y (2022). Application of machine learning, deep learning and optimization algorithms in geoengineering and geoscience: Comprehensive review and future challenge. *Gondwana Research*, 109: 1-17.
- [Zhou et al. 2020] Zhou, Yuekuan, Siqian Zheng, and Guoqiang Zhang (2020). Machine-learning based study on the on-site renewable electrical performance of an optimal hybrid PCMs integrated renewable system with high-level parameters' uncertainties. *Renewable Energy*, 151: 403-418.
- [Zhu et al. 2020] Zhu R, Hu X, Hou J, Li X (2020). Application of machine learning techniques for predicting the consequences of construction accidents in China. *Process Safety and Environmental*

Protection, 145: 293-302.